Photoelectron diffraction study of ultrathin Fe films on Cu{111}

A. Theobald, O. Schaff, C. J. Hirschmugl, V. Fernandez, K.-M. Schindler, M. Polcik,* and A. M. Bradshaw
Fritz-Haber-Institut der Max-Planck-Gesellschaft, Faradayweg 4-6, 14195 Berlin-Dahlem, Germany

D. P. Woodruff
Department of Physics, University of Warwick, Coventry CV4 7AL, England
(Received 5 June 1998)

Using photoelectron diffraction in the scanned-energy mode we show that at 300 K iron grows pseudomorphically on Cu{111} up to a thickness of about two equivalent monolayers. The Fe-Cu layer separation is 1.99 Å. Above this thickness the film becomes bcc with {110} orientation and is aligned such that the ⟨111⟩ rows are parallel to the ⟨110⟩ rows of the fcc{111} surface (Kurdjumov-Sachs orientation). The Fe-Fe first-layer separation is 1.95 Å. [S0163-1829(99)01903-7]

I. INTRODUCTION

Ultrathin films of metastable fcc, or γ-, iron can be prepared epitaxially on fcc metal single-crystal surfaces up to thicknesses of a few monolayer equivalents (MLE),[1–14] even though the lattice constant of the substrate may not match exactly that of the iron. The necessary conditions for this so-called pseudomorphic growth are that the surface energy of the overlayer should be lower than that of the substrate and that the lattice mismatch is indeed quite small. Because the lattice parameter of γ-iron (3.59 Å, when extrapolated from above the martensitic transition at 1183 K down to room temperature) is very close to that of Cu (3.61 Å), the latter has proved to be a suitable substrate material. Because of the rich variety of magnetic behavior of γ-iron depending on its lattice constant, there has been considerable interest in the magnetic properties of iron films grown on Cu.[15–17] While on Cu{100} a high-spin, tetragonally distorted phase as well as a low-spin fcc phase have been observed,[16] on Cu{111} the thermally deposited films show low-spin ferromagnetic or ferrimagnetic phases.[15] Structural studies have recently been extended to thin films of Mn, Cr, and Co.[18–27] Most studies have been concerned hitherto with the pseudomorphic growth of Fe on Cu{100}, a system for which rather detailed structural studies have been published (see Refs. 2, 7, 10, and 11, and references therein). Less attention has been paid to the ultrathin Fe films that can be grown on Cu{111}. In an early low-energy electron diffraction (LEED) and Auger study of this system Gradmann *et al.*[28] reported layer-by-layer growth of ''completely pseudomorphic'' γ-Fe to a thickness of about 10 Å followed by island growth to at least several tens of Å. For thicker films the LEED pattern gradually changed to that corresponding to normal (bcc) α-Fe{110}, such that the close-packed ⟨111⟩ rows of the bcc crystal are parallel to the close-packed ⟨110⟩ rows of the fcc(111) surface. This is known as the Kurdjumov-Sachs (KS) orientation and is shown schematically in Fig. 1. Another possibility would be the Nishiyama-Wasserman (NW) orientation for which the ⟨100⟩ bcc direction is parallel to fcc ⟨110⟩. Quantitative LEED studies were performed for films of thicknesses 1 and 5 MLE by Darici *et al.*[1] and Tian *et al.*,[5] respectively, who also found pseudomorphic growth. Using forward-scattering x-ray photoelectron diffraction (XPD) Kief and Egelhoff[6,19] established that there are two temperature-dependent growth modes. At 80 K the iron layer has the bcc structure, but at 300 K it grows initially fcc and then relaxes to bcc at a thickness between 3 and 6 MLE. The data also showed that the bcc film has the KS orientation, as did the LEED work of Tian *et al.*[5] At both temperatures nearly layer-by-layer growth was found to occur. Scanning tunneling microscopy has shown that in the submonolayer regime an island structure is formed.[8] The low-energy ion-scattering data of Detzel and Memmel[29] have indicated that surface segregation of Cu to the surface of the iron film occurs for growth at 300 K. Similar results have recently been obtained for Co layers on the same substrate.[22]

We have previously shown that photoelectron diffraction (PhD) in the scanned-energy mode can be useful for studying the very early stages of metallic-film growth.[14,25] In this experiment the intensity of an (adsorbate) core-level photoemission line is measured as a function of photon energy, and thus of photoelectron kinetic energy, at a fixed-emission angle.[30] The observed-intensity modulations are due to the interference of the component of the photoelectron wave that

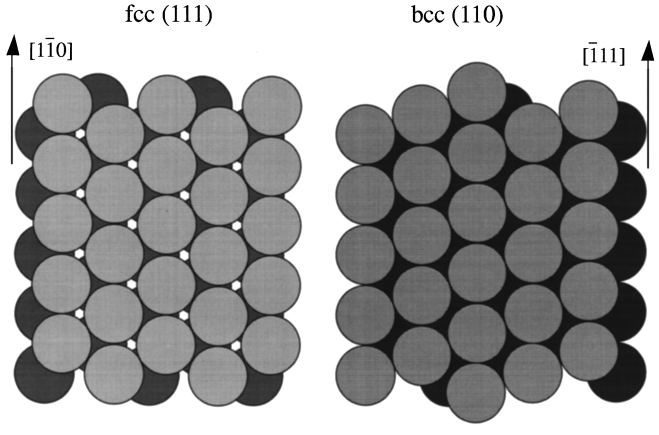

FIG. 1. Schematic diagram showing the relative azimuthal alignment of an fcc(111) substrate (left) and bcc(110) overlayer (right) in the Kurdjumov-Sachs orientation.

reaches the detector directly with those components that are first scattered from neighboring atoms. The path-length differences that reflect both the direction and separation of the neighboring scatterers from the emitter atom thus contain information on the local structure. Notice that this approach picks out the backscattering scattering paths (true forward zero-degree scattering involves no path-length difference) and so provides information especially on the emitter location relative to the underlying substrate. By contrast, the higher-electron kinetic-energy angle-scan XPD experiments mentioned above[6,19] provide information mainly on the forward-scatterer atoms that lie above the emitter. In order to extract the structure information the intensity modulations are simulated with a multiple-scattering computer code for various model structures in a trial-and-error procedure. Long-range order in the overlayer is not a necessary prerequisite, although the presence of more than two different local geometries, e.g., two different adsorption sites, does complicate the data analysis and increases the probability of ambiguities or reduced precision in the resulting structure.

In the present paper we describe a scanned energy-mode photoelectron-diffraction study of the system Cu{111}-Fe, which confirms essentially the forward-scattering result at 300 K, but also gives quantitative structural information on the ultrathin films.

II. EXPERIMENTAL DETAILS AND DATA ANALYSIS

The PhD data were recorded in a purpose-built ultrahigh vacuum system on the HE-TGM-1 monochromator[31] at the Berlin synchrotron radiation source BESSY. A 152 mm mean radius 150° electrostatic deflection analyzer with three parallel channeltrons (VG Scientific) was used to measure the signal at a fixed angle of 60° relative to the photon-incidence direction. The Cu{111} sample was prepared by the usual methods of orientation with Laue x-ray diffraction, spark machining, polishing, and *in situ* cleaning with argon bombardment and anneal cycles. A well-defined (1×1) LEED pattern was then observed; atomic cleanliness was monitored with core-level photoelectron spectroscopy using synchrotron radiation. The iron films were evaporated onto the substrate at 130 and 300 K. The Fe $2p_{3/2}$ photoelectron-diffraction spectra for 0.4 MLE at 300 K were taken at polar emission angles between $-10°$ and 50° in the $\langle 110\rangle$ azimuth and the two $\langle 211\rangle$ azimuths in 10° steps. Further modulation functions at 1.1, 2.5, and 4.9 MLE were measured in the five emission directions, which showed the strongest modulations at 0.4 MLE. Although deposition took place at 300 K, the sample was cooled to 130 K in order to take the diffraction data. At a deposition temperature of 130 K quantitative measurements were made in altogether 13 different emission directions. The Fe $2p_{3/2}$ core-level signal was recorded in photon-energy steps of 2 eV for kinetic energies of about ± 20 eV around the Fe $2p_{3/2}$ core-level peak to give the energy distribution curves. The intensity of each of these peaks was then determined by background subtraction and integration, and the resulting intensity-energy spectra between 80 and 450 eV were normalized to give the modulation functions:[32]

$$\chi_{\mathrm{ex}}(\theta,\phi,k)=[I(k)-I_0(k)]/I_0(k), \tag{1}$$

where I and I_0 are the diffractive and nondiffractive intensity, θ and ϕ are the polar and azimuthal emission angles, and k is the modulus of the photoelectron wave vector.

The commercial-evaporation source (Omicron) contained a piece of iron wire (purity 99.99%) heated by electron bombardment. The evaporation rate, which could be monitored by the ion current at the exit tube, was held constant at typically 0.0045 MLE s^{-1} during an experiment. It was calibrated by measuring the attenuation of the Cu $3p$ substrate signal as a function of time at coverages $\ll 1$ MLE. One can easily show that for the growth of a monolayer,[33]

$$I/I_0=1-(1-s)at. \tag{2}$$

$s=\exp(d/\lambda)$, where λ is the mean free path for inelastic electron scattering in iron, a the arrival rate, and $\Theta(\text{in MLE})=at$. For the other extreme, namely, growth in islands of uniform thickness Nd,

$$I/I_0=1-(1-s^N)a_N t/N. \tag{3}$$

a_N is the upper boundary for the rate of arrival of Fe atoms at the substrate surface. In the case of Volmer-Weber growth the attenuation of the substrate signal with time will be more complicated, falling (at least for <1 MLE) between the two straight lines given by Eqs. (2) and (3). At very low coverages, however, it will be almost linear and virtually identical with that given by Eq. (2). The latter can then be used to calibrate the evaporation rate, and thus to determine all other, higher coverages. The main source of error in the coverage determination lies in the value for λ, which has to be taken from the literature. In the case of Cu{100}-Mn (Ref. 25) LEED patterns could be used for additional calibration. Using Eq. (2) there was agreement to within a few percent for the point at which the half-order diffraction features associated with the $(\sqrt{2}\times\sqrt{2})R45°$-Mn structure have their maximum intensity at 0.5 MLE. In general, however, the uncertainty in λ may be as high as 25%, which is also the upper limit for the error in the thickness. In the present study we have used an interpolated value for λ of 14.3 Å for iron at 860 eV, as given by Tanuma *et al.*[34]

III. SIMULATIONS

In the Berlin-Warwick approach to quantitative-photoelectron diffraction,[30,32] structure determination generally proceeds in two stages. The projection method[35] is first used to determine the adsorption site. This consists of an ''inversion'' of the experimental data to produce a real-space image of the near-neighbor backscatterers surrounding the emitter. The underlying physical principle is that modulation functions recorded in directions that correspond to 180° scattering from a near-neighbor substrate atom show particularly strong modulations. Under these circumstances the modulation function is dominated by this single-scattering event, and the periodicity can be described by taking only one scatterer into account. The method produces a three-dimensional intensity map of the space around the emitter, with maximum values of the ''projection integral'' in regions corresponding to the nearest-neighbor backscatterers. This stage thus provides a valuable first indication of the most probable local-adsorption site for subsequent optimization.

The second stage is a true quantitative-structural analysis

using an iterative ''trial-and-error'' procedure, which involves a comparison of a reduced set of usually six to eight experimental spectra with the results of full multiple-scattering simulations based on trial-model structures. These calculations are performed on the basis of an expansion of the final-state wave function into a sum over all scattering pathways, which the electron can take from the emitter atom to the detector outside the sample. A magnetic quantum-number expansion of the free-electron propagator is used to calculate the scattering contribution of an individual-scattering path.[36] Double- and higher-order scattering events are treated by means of the reduced angular momentum expansion.[37] The finite-energy resolution and angular acceptance of the electron analyzer are included. Anisotropic vibrations for the emitter atom and isotropic vibrations for the scattering atoms are also taken into account. The comparison between theory and experiment is quantified by the use of an objective reliability factor

$$R_{\mathrm{m}}=\sum\ (\chi_{\mathrm{th}}-\chi_{\mathrm{ex}})^2 \Big/ \sum\ (\chi_{\mathrm{th}}^2+\chi_{\mathrm{ex}}^2), \tag{4}$$

where a value of 0 corresponds to perfect agreement, a value of 1 to uncorrelated data, and a value of 2 to anticorrelated data.[30,32] The search in parameter space to locate the structure having the minimum R factor was helped by the use of a Marquardt algorithm, in which the calculation of the curvatures is made considerably faster by using the so-called linear method.[38]

In order to estimate the errors associated with the individual structural parameters we use an approach based on that of Pendry, which was derived for LEED.[39] This involves defining a variance in the minimum of the R factor R_{min} as

$$\mathrm{Var}(R_{min})=R_{min}\sqrt{(2/N)}, \tag{5}$$

where N is the number of independent pieces of structural information contained in the set of modulation functions used in the analysis. All parameter values giving structures with R factors less than $R_{min}+\mathrm{Var}(R_{min})$ are regarded as falling within one standard deviation of the ''best fit'' structure. More details of this approach, and in particular the definition of N, can be found in a recent publication.[40]

IV. RESULTS AND DISCUSSION

A set of normal-emission modulation functions for Fe films deposited at a substrate temperature of 300 K corresponding to thicknesses of 0.4, 1.1, 2.5, and 4.9 MLE is shown in Fig. 2. The modulation amplitude of $\sim\pm0.2$ is typical for each of the five identical emission directions measured for each thickness. The 0.4 and 1.1 MLE normal-emission spectra of Fig. 2 are very similar to each other, as are those at 2.5 and 4.9 MLE. Between 1.1 and 2.5 MLE, however, the modulation function clearly changes its form, indicating that a change in the structure of the iron film takes place. Similar differences were found for the modulation functions measured at other emission angles (see Sec. II). Apart from an increase in the diffuse background, the (1×1) LEED pattern remained essentially unaltered during the change in structure. We note that previous studies of this system indicate a structural transition with increasing coverage from fcc to bcc: Kief and Egelhoff[6,19] identify this transition as occurring between 3 and 6 MLE, while Tian *et al.*[5] certainly found the bcc structure at 13 MLE. In the present paper detailed structural analyses were carried out for the 0.4 and 4.9 MLE Fe films, which appear to typify the low- and high-coverage regimes in our experiments.

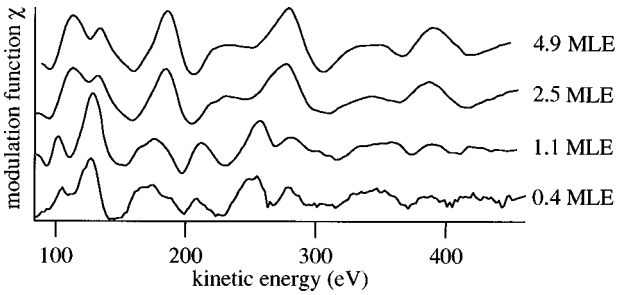

FIG. 2. Normal-emission modulation functions for Fe layers on Cu{111} of different thickness prepared at room temperature. Note the change in the modulation functions between 1.1 and 2.5 MLE.

In the first step of the analysis of the 0.4 MLE data the projection method[35] was first applied in order to establish the most probable adsorption site. The projection integrals were calculated using the full-data set, although this is not actually necessary: as few as five or six modulation functions are normally sufficient. The result is shown in Fig. 3 in the form of gray-scale maps of cuts (a) perpendicular to the surface passing through the Fe emitter [located at (0,0,0)] in a $\langle211\rangle$ azimuth, and (b) parallel to the surface at an appropriate distance below (2.0 Å) so as to intersect the feature seen in the perpendicular cut. Dark regions correspond to maxima in the value of the projection integral and indicate the most probable locations of backscatterers, in this case the Cu atoms (or possibly other Fe atoms) forming the adsorption site. The crescentlike shape of the ''images'' of the substrate atoms is an artifact of the method.[35] The clear inference to be drawn from Fig. 3 is that the Fe atom is situated in a threefold symmetric site. Moreover, because of the azimuthal orientation of the pattern relative to the known crystallographic directions, it can be immediately concluded that it is the fcc site (directly above a third-layer atom), which is occupied. Even in this first stage of the analysis it is, therefore, apparent that pseudomorphic growth occurs. Note that the projection method is not able to distinguish between layer growth

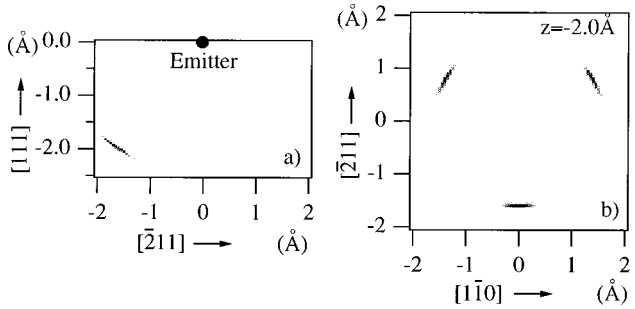

FIG. 3. Results from the application of the projection method to the 300 K Cu{111}-Fe system at 0.4 MLE. Film deposition took place at a substrate temperature of 300 K. Cuts (a) perpendicular to the surface in a $\langle211\rangle$ azimuth and (b) parallel to the surface 2.0 Å below the emitter are shown.

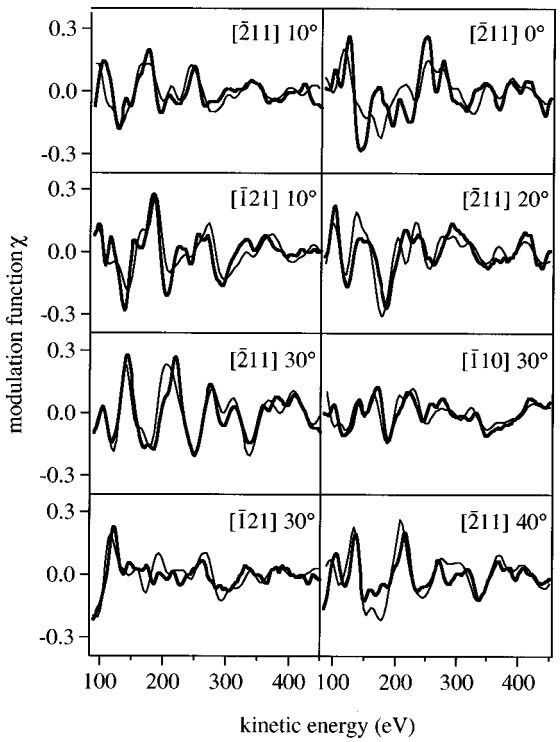

FIG. 4. Bold curves: Fe $2p_{3/2}$ modulation functions measured in eight different directions for a 0.4 MLE iron layer deposited on a Cu{111} surface at 300 K. Light curves: multiple scattering simulations for an iron monolayer.

and island growth. Although the backscattering from Cu atoms is implicitly assumed in the calculation of the projection integrals, the scattering factors for Fe and Cu are sufficiently similar that an ''adsorption site'' consisting of Fe atoms at the outer layer of a pseudomorphic Fe island would give the same result.

The full-scale simulations were carried out by comparison with the eight experimental modulation functions shown in Fig. 4 (bold lines). The polar angle of emission and the crystal azimuth are given in each case. Three different model structures were tested, each assuming occupation of fcc hollow sites: a Fe monolayer, a Fe bilayer, and a Cu-Fe-Cu sandwich structure consisting of a Fe monolayer with a Cu monolayer on top. Figure 5 defines the structural parameters varied in the simulations; the Fe monolayer is used as the example. The best R factor of 0.25 was obtained for the monolayer with a variance of 0.04. The values for the bilayer and the sandwich structure were 0.31 and 0.40, respectively, both of which are clearly outside the variance. The agreement for the sandwich structure is so poor that we will not consider it further here, although we note that low-energy

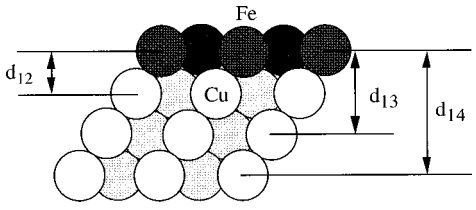

FIG. 5. The structural parameters used in the multiple-scattering simulations to fit the experimental modulation functions.

TABLE I. Measured interlayer spacings for thin Fe films deposited on Cu{111} at 300 K.

Parameter	Value (Å)	
0.4 MLE (fcc)	monolayer	bilayer
d_{12}	1.99(3)	1.99(5)
d_{13}	4.12(7)	4.09(7)
d_{14}	6.62(20)	6.23(17)
4.9 MLE (bcc; Kurdjumov-Sachs orientation) thick film		
d_{12}	1.95(6)	
d_{13}	3.98(3)	

ion scattering shows some evidence for segregation of Cu atoms to the surface of the iron film at 300 K.[29] We return to the bilayer model below. The calculated ''best-fit'' modulation functions for the monolayer are shown as faint curves in Fig. 4. Whereas the agreement is not perfect, most of the major features are reproduced by the calculation, as indicated by the moderately good R factor of 0.25.

The optimum values of the three structural parameters for both the monolayer and bilayer are given in Table I. The Fe-Cu layer spacing d_{12} is 1.99($\pm$0.03) Å for the monolayer, which is slightly smaller than the Cu-Cu layer spacing of 2.04($\pm$0.02) Å for clean Cu{111}.[1] We note that the values for d_{12} are identical for the monolayer and bilayer and that in the case of d_{13} and d_{14} they are also very similar, lying within their respective precisions estimates. In this situation it is appropriate to consider a third possibility, namely, the coexistence of monolayer and bilayer regions, simply by adding the modulation functions of the two with different weightings and determining the R factor by comparison with the experimental data of Fig. 4. (Strictly one should perform a separate structural optimization for each monolayer/bilayer ratio, but this involves a huge computational effort and was felt to be inappropriate.) The result is shown in Fig. 6(a) in which the R factor is plotted against the percentage of bilayer islands. The minimum occurs for a bilayer fraction of below 10%. A parabola has been fitted to the calculated points and reaches $R=0.29$, the value of the lowest R factor plus its variance, at a bilayer fraction of 78%. The pure monolayer thus remains the most probable structure for the Fe film at 0.4 MLE thickness, but the presence of the bilayer regions covering up to almost 80% of the surface cannot be excluded. If a significant fraction of the surface were to be covered with bilayers, a small proportion of trilayer regions might also be expected, but this possibility was not tested, again because of the huge computational effort involved. Based on the data listed in Table I, the atomic volume of the bilayer is $V_a=11.3(\pm 0.3)$ Å^3, which is only slightly less than that for γ-iron (lattice parameter 3.59 Å) of 11.6 Å^3. These values correspond to the antiferromagnetic state.[11]

Although the results of the projection method imply occupation of the fcc sites alone, the method is designed to pick out only the strongest scatterer contributions, and in the case of multiple-site occupations it suppresses information from any ''minority species.'' The specific possibility of partial occupation of fractional occupation of hcp hollow sites (directly above second-layer atoms) was therefore tested. In this case a full optimization of both the ratio of fcc and hcp site occupation and the local geometry of each site was per-

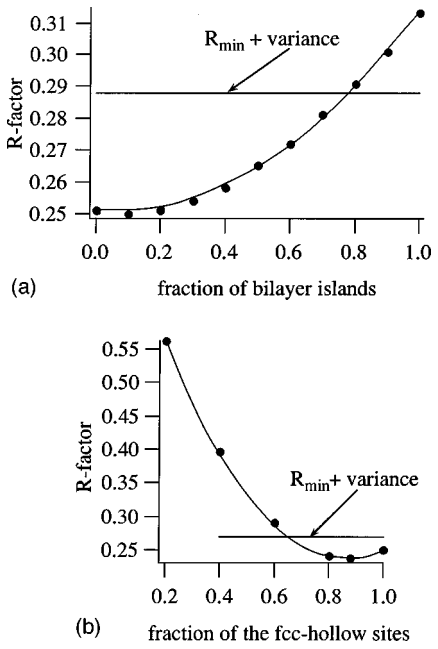

FIG. 6. (a) R factor as a function of the bilayer/monolayer ratio for the 0.4 MLE Fe film on Cu{111}. The intersection of the parabolic fit through the points and the variance in the R factor yields the precision. (b) R factor as a function of the fractional fcc/hcp site occupation in a monolayer for the system Cu{111}-Fe at 0.4 MLE.

formed. The result is shown in Fig. 6(b) in which the R factor is plotted as a function of the relative percentage of fcc/hcp site occupation. The minimum in the R factor of 0.24 occurs for 12% hcp sites. Complete occupation of hcp sites corresponds to an R factor in excess of 0.80, which is clearly unacceptable. The horizontal line corresponding to an R factor of R_{min} plus the variance (0.04) intersects the parabola at the 33% hcp site occupation. Therefore, the most probable structure of the monolayer has 88% of the Fe atoms in fcc sites, although a lower limit of 67% is theoretically possible. We note, however, that 100% fcc site occupation—perhaps the expected result—is well within the error estimate.

We now turn our attention to the film of 4.9 MLE thickness. In this case the projection method did not give a result compatible with adsorption on a highly symmetric adsorption site on a Cu{111} surface. The only feature was a diffuse structure about 2.2 Å directly beneath the emitter, which is probably an artifact associated with the sum of many different near-neighbor directions rather then a simple atop geometry. In consequence, three specific structures were simulated, namely, a thick (>10 MLE) pseudomorphic film as well as thick (>10 MLE) bcc{110} films in both the KS and NW orientations. Whereas the R factor for the pseudomorphic film was over 0.6, the result for the KS-bcc film was 0.18 and for the NW-bcc film 0.21. With a variance of 0.05 the NW orientation cannot be excluded on the basis of the photoelectron-diffraction data alone. However, the fact that only the KS orientation is observed in LEED for thicker films is a very strong indication that this geometry is adopted. The good agreement between the simulated and measured modulation functions for the KS orientation is shown in Fig. 7. The structural parameters varied were the layer distances d_{12} and d_{13} (see for example Fig. 5); the results are given in Table I. d_{12} exhibits a contraction of

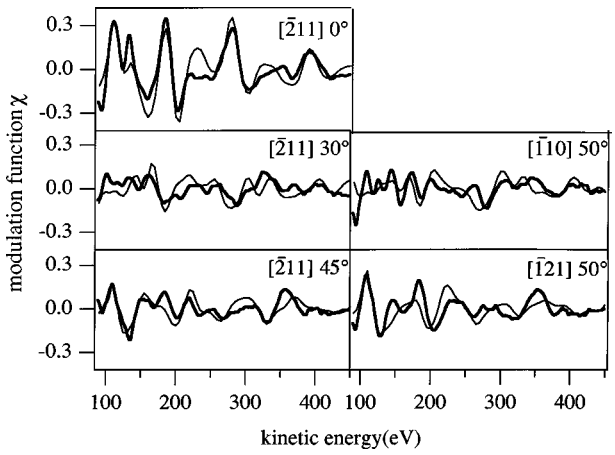

FIG. 7. Bold curves: Fe $2p_{3/2}$ modulation functions in five different directions for a 4.9 MLE iron layer deposited on a Cu{111} surface at 300 K. Light curves: multiple-scattering simulations for bcc iron (>10 layers) in the Kurdjumov-Sachs orientation.

$4(\pm 2)\%$ relative to the bulk-layer spacing of 2.03 Å. A d_{12} value of 2.04 Å has been found with LEED for the surface of a bulk {110} single crystal.[41] We note that the error bars on d_{13} are actually smaller than on d_{12}. This is due to the fact that on Fe{110} there is a substrate atom directly below the emitter in the third layer, so that normal emission is a strong backscattering direction, giving rise to strong intensity modulations. Perhaps more important, however, is the fact that normal emission is the only direction in which all the six domains of this structure have identical modulation functions. The corresponding parameters obtained to form the ''best-fit'' structure for the NW orientation were $d_{12} = 1.97(\pm 0.06)$ Å and $d_{13} = 3.98(\pm 0.03)$ Å.

Finally, we consider the results of the experiments involving deposition at a sample temperature of 130 K. The 0.4 MLE Fe films prepared at this temperature also show relatively strong modulations, which in some directions (e.g., normal emission, [$\bar{1}$10]) are very similar to the result obtained from the film grown at 300 K. In other directions, however, there is little or no agreement in the energies of the main maxima and minima (e.g., 40°, [$\bar{1}\bar{2}$1]). In yet further directions there is relatively good agreement in the peak energies, but the modulation amplitudes are considerably smaller in the 130 K case (e.g., 20°, [$\bar{2}$11]). Calculations based on several simple model structures all led to high R-factor values. The lowest R factor of 0.38 was actually obtained for the unlikely twofold symmetric bridge site. We conclude that either no well-defined adsorption site exists, or more likely, that two or more phases are present.

In summary, we note that the 300 K results are in good agreement with Kief and Egelhoff[6,19] and Tian *et al.*,[5] the only major difference being the thickness at which the relaxation from the pseudomorphic fcc structure to the bcc structure of bulk iron takes place. In the former study using scanned angle-mode photoelectron diffraction the critical thickness was determined to lie between 3 and 6 MLE. Tian *et al.* in a LEED study found the thickness to lie around 7 MLE. The present value of ~ 2 MLE is considerably lower; we estimate our precision to be no worse than about 25% and, as explained above, this is due almost entirely to the

uncertainty in the inelastic scattering mean free path. Kief and Egelhoff used an indirect method (CO titration) to estimate their coverage, while Tian *et al.*[5] measured the ratio of the Auger peaks $I_{Fe}(651\ eV)/I_{Cu}(920\ eV)$. Their estimated error in the film thickness was $\pm 50\%$. There may also have been small, but perhaps, important differences in temperature between the various measurements. Our results are in good agreement with a more recent LEED study[15] where the critical thickness was also found between 2.3 and 2.7 MLE of Fe on Cu{111}. The significance of the present scanned-energy mode photoelectron-diffraction measurements lies not only in the confirmation of the previously reported relaxation of the fcc phase into the bcc phase as a function of thickness at 300 K, but also in the quantitative determination of the most important structural parameters. The discrepancies at 130 K are more difficult to explain: Kief and Egelhoff reported immediate bcc growth at 80 K, which is clearly not consistent with our data.

V. CONCLUSIONS

Using scanned energy-mode photoelectron diffraction we have examined the thin Fe films formed on Cu{111} by deposition at sample temperatures of 300 and 130 K. The modulation functions measured at various angles as a function of coverage following deposition at 300 K show that the Fe atoms retain the local geometry of the Cu substrate up to about two equivalent monolayers, i.e., the film grows pseudomorphically in the fcc structure. A monolayer is the most probable structure for the thinnest film studied (0.4 MLE), but partial coverage by islands of bilayer or even trilayer thickness are possible. A structure based entirely on bilayer islands can, however, be ruled out. The Fe-Cu layer separation in the case of the monolayer is $1.99(\pm 0.03)$ Å. Above a thickness of about two equivalent monolayers the fcc film converts into the bcc{110} structure with the Kurdjumov-Sachs orientation. The Fe-Fe first-layer separation is $1.95(\pm 0.06)$ Å. In neither case is there any evidence for the segregation of Cu to the surface of the Fe film. At 130 K no structural determination was possible, although the data showed relatively strong modulations. The data are, however, definitely not consistent with either pure pseudomorphic growth or pure bcc island growth; most probably, more than one Fe phase grows on the surface.

ACKNOWLEDGMENTS

The authors are pleased to acknowledge financial support of this work in the form of grants from the Deutsche Forschungsgemeinschaft through the Sonderforschungsbereich 290, the Federal Ministry for Education, Science, Research and Technology (Germany) under Contract No. 05 625 EBA 6, the Engineering and Physical Sciences Research Council (U.K.) and the European Union through a Human Capital and Mobility network (No. ERBCHRX CT930358), and the Large-Scale Facilities Program.

*Also at Institute of Physics of the Academy of Sciences of the Czech Republic, Cukrovarnicka 10, 162 53 Prague, Czech Republic.

[1] Y. Darici, J. Marcano, H. Min, and P. A. Montano, Surf. Sci. **195**, 566 (1988).
[2] S. H. Lu, J. Quinn, D. Tian, F. Jona, and P. M. Marcus, Surf. Sci. **209**, 364 (1989).
[3] C. Liu and S. D. Bader, J. Vac. Sci. Technol. A **8**, 2727 (1990).
[4] S. H. Lu, Z. Q. Wang, D. Tian, Y. S. Li, F. Jona, and P. M. Marcus, Surf. Sci. **221**, 35 (1991).
[5] D. Tian, F. Jona, and P. M. Marcus, Phys. Rev. B **45**, 11 216 (1992).
[6] M. T. Kief and W. F. Egelhoff, Jr., J. Vac. Sci. Technol. A **11**, 1661 (1993).
[7] M. Wuttig and J. Thomassen, Surf. Sci. **282**, 237 (1993).
[8] A. Brodde, K. Dreps, J. Binder, Ch. Lunau, and H. Neddermeyer, Phys. Rev. B **47**, 6609 (1993).
[9] H. J. Elmers and J. Hauschild, Surf. Sci. **320**, 134 (1994).
[10] K. Heinz, S. Müller, and P. Bayer, Surf. Sci. **337**, 215 (1995).
[11] S. Müller, P. Bayer, C. Reischl, K. Heinz, B. Feldmann, H. Zillgen, and M. Wuttig, Phys. Rev. Lett. **74**, 765 (1995).
[12] H. Bethge, D. Heuer, Ch. Jensen, K. Reshöft, and U. Köhler, Surf. Sci. **331-333**, 878 (1995).
[13] G. W. Anderson and P. R. Norton, Surf. Sci. **336**, 262 (1995).
[14] A. Theobald, S. Bao, V. Fernandez, K.-M. Schindler, O. Schaff, V. Fritzsche, A. M. Bradshaw, N. Booth, and D. P. Woodruff, Surf. Sci. **385**, 107 (1997).
[15] J. Shen, M. Klaua, P. Ohresser, H. Jenniches, J. Barthel, Ch. Mohan, and J. Kirschner, Phys. Rev. B **56**, 11 134 (1997).
[16] M. Zharnikov, A. Dittschar, W. Kuch, C. M. Schneider, and J. Kirschner, J. Magn. Magn. Mater. **174**, 40 (1997).
[17] J. Shen, P. Ohresser, Ch. V. Mohan, M. Klaua, J. Barthel, and J. Kirschner, Phys. Rev. Lett. **80**, 1980 (1998).
[18] M. Wuttig, Y. Gauthier, and S. Blügel, Phys. Rev. Lett. **70**, 3619 (1993).
[19] M. T. Kief and W. F. Egelhoff, Jr., Phys. Rev. B **47**, 10 785 (1993).
[20] H. P. Noh, T. Hashizume, D. Jeon, Y. Kuk, H. W. Pickering, and T. Sakurai, Phys. Rev. B **50**, 2735 (1994).
[21] M. E. Haugan, Qibiao Chen, and M. Onellion, Phys. Rev. B **49**, 14 028 (1994).
[22] A. Rabe, N. Memmel, A. Steltenpohl, and Th. Fauster, Phys. Rev. Lett. **73**, 2728 (1994).
[23] V. Scheuch, K. Potthast, B. Voigtländer, and H. P. Bonzel, Surf. Sci. **318**, 115 (1994).
[24] D. Rouyer, C. Krembel, M. C. Hanf, D. Blomont, and G. Gewinner, Surf. Sci. **331-333**, 957 (1995).
[25] R. Toomes, A. Theobald, R. Lindsay, T. Gießel, O. Schaff, R. Didszuhn, D. P. Woodruff, A. M. Bradshaw, and V. Fritzsche, J. Phys.: Condens. Matter **8**, 10 231 (1996).
[26] S. Müller, G. Kostka, T. Schäfer, J. de la Figuera, J. E. Prieto, C. Ocal, R. Miranda, K. Heinz, and K. Müller, Surf. Sci. **352-354**, 46 (1996).
[27] S. K. Kim, F. Jona, and P. M. Marcus, Surf. Sci. **349**, 160 (1996).
[28] U. Gradmann, W. Kümmerle, and P. Tillmanns, Thin Solid Films **34**, 249 (1976); U. Gradmann and P. Tillmanns, Phys. Status Solidi A **44**, 539 (1977).
[29] Th. Detzel and N. Memmel, Phys. Rev. B **49**, 5599 (1994).
[30] D. P. Woodruff and A. M. Bradshaw, Rep. Prog. Phys. **57**, 1029 (1994).
[31] E. Dietz, W. Braun, A. M. Bradshaw, and R. L. Johnson, Nucl. Instrum. Methods Phys. Res. A **239**, 359 (1985).

[32] Ph. Hofmann, K.-M. Schindler, S. Bao, V. Fritzsche, A. M. Bradshaw, and D. P. Woodruff, Surf. Sci. **337**, 169 (1995).
[33] R. Sinda, Surf. Sci. **140**, 472 (1984).
[34] S. Tanuma, C. J. Powell, and D. R. Penn, Surf. Interface Anal. **17**, 1 (1991).
[35] Ph. Hofmann and K.-M. Schindler, Phys. Rev. B **47**, 13 941 (1993); Ph. Hofmann, K.-M. Schindler, S. Bao, A. M. Bradshaw, and D. P. Woodruff, Nature (London) **368**, 131 (1994).
[36] V. Fritzsche, J. Phys.: Condens. Matter **2**, 1413 (1990); Surf. Sci. **265**, 187 (1992).
[37] V. Fritzsche, Surf. Sci. **213**, 648 (1986).
[38] V. Fritzsche and J. B. Pendry, Phys. Rev. B **48**, 9054 (1993).
[39] J. B. Pendry, J. Phys. C **13**, 937 (1980).
[40] N. A. Booth, R. Davis, R. Toomes, D. P. Woodruff, C. Hirschmugl, K.-M. Schindler, O. Schaff, V. Fernandez, A. Theobald, Ph. Hofmann, R. Lindsay, T. Gießel, P. Baumgärtel, and A. M. Bradshaw, Surf. Sci. **387**, 152 (1997).
[41] H. D. Shih, F. Jona, U. Bardi, and P. M. Marcus, J. Phys. C **13**, 3801 (1980).